THEORY OF LIGHT DIFFRACTION BY SINGLE SKELETAL MUSCLE FIBERS

Y. YEH, *Department of Applied Science, University of California, Davis, California 95616*
R. J. BASKIN AND R. L. LIEBER, *Department of Zoology, University of California, Davis, California 95616*
K. P. ROOS, *Cardiovascular Research Laboratory, UCLA School of Medicine, Los Angeles, California 90024 U.S.A.*

ABSTRACT A theoretical discussion is presented describing the diffraction of laser light by a single fiber of striated muscle. The complete three-dimensional geometry of the fiber has been taken into consideration. The basic repeated unit is taken as the sarcomere of a single myofibril, including its cylindrical geometry. The single fiber is considered as the sum of myofibrils up to the fiber dimensions. When proper phasing is taken into account, three cases of interest are analyzed. (*a*) When the adjacent myofibrils are totally aligned with respect to their index of refraction regions (e.g., A and I bands), then the diffraction pattern reflects that of a larger striated cylinder with the dimensions of the fiber. (*b*) When a particular skew plane develops for the myofibril elements, additional Bragg reflection occurs at certain specific sarcomere lengths, and intensity asymmetry amongst the diffracted orders occurs. (*c*) When the myofibril phasing changes in a random fashion, while all sarcomeres remain at the same length, then intensity decrease is directly related to the phase deviation from a reference phase point. This condition may well describe a fiber undergoing active isometric contraction.

INTRODUCTION

Recent experimental studies on the light diffraction pattern by single fibers of striated muscles point toward two important features: Baskin et al. (1), showed that a three-dimensional cylindrical grating is necessary to describe the first and second order symmetrical intensity patterns as a function of the passively stretched length. It was also shown by these authors that the inclusion of other elements in the consideration of the grating (e.g., the Z-membrane and the H-band) can lead to improvement in the correspondence between theory and experiment. Rudel and Zite-Ferency (2) further strengthened the idea that three-dimensional grating consideration is vital for the interpretation of single fiber data by showing that Bragg reflection by the lattice composed of skewed myofibril elements is essential to the observed asymmetrical intensity pattern between left and right diffraction order maxima. These authors (3) suggested that such Bragg effect over different regions of the sarcomeres, each with its own Bragg orientation, allows for an interpretation of the stepwise pauses in the position of the peak of the first order line during shortening, as observed by Pollack, et al. (4).

That a planar or linear grating as a model for muscle fiber diffraction is inadequate seems clear. Fujime and Yoshino (5) also recently discussed the three-dimensionality of the fiber grating and improved upon their previous theoretical predictions (6).

The present paper will continue to deal with idealized cases of myofibril bundles. The emphasis will be to examine what additional features are reflected in the diffraction patterns

when either myofibril skewness or myofibril randomness is considered. For the case of systematic myofibril skewness, the conditions for observing symmetrical and asymmetrical diffraction patterns will be presented. It will also be shown that for a given sarcomere length, relative intensities of different diffraction orders undergo fairly dramatic changes as a function of skewness.

For the case of random phasing of the myofibrils, the present work shows that a decrease in diffraction intensity at each order, accompanied by changes in the intensity profile within any azimuthal plane, will take place.

THEORY

Three fundamental features of a single fiber will each cause distinctive diffraction patterns for incident monochromatic light: (*a*) the sarcomere periodicity within a myofibril; (*b*) the basic cylindrical nature of the myofibril or fiber; (*c*) the linear misalignment of the myofibril elements relative to a given reference myofibril. In considering such a complex geometrical configuration for diffraction, we have chosen to use the more basic formalism where diffraction is considered the result of light being scattered from a striated cylindrical medium with a periodicity Λ, the sarcomere length. For the essential aspects of the light-sarcomere interaction to be fully appreciated, the single scattering case is treated in detail. We will discuss the multiple scattering results in a later section. Within the limits of these approximations, the intensity of detected light at any point of observation is the square of the sum of the electric field contribution from each and every element of the scatterer, including all aspects of its phase regularity in the index of refraction.

Consider the geometry of Fig. 1, where the cylinder is aligned along the **z**-axis, and the incident light, polarized along the **x**-axis, $\hat{n}_0$, is propagating along the **y**-axis, with wave vector $\mathbf{k}_0$. Here, $\hat{n}_0$ is the unit incident polarization vector, while $|k_0| = 2\pi n_0/\lambda_0$, λ_0 being the incident wavelength in vacuum and n_0 the average material index of refraction. If the material of the cylinder has a macroscopic dielectric fluctuation function $\delta\bar{\epsilon}(\mathbf{r})$, where $\mathbf{r}$ is within the cylinder volume, then within the framework of this dipole approximation, the scattered field at point $\mathbf{R}$ is given by (7)

$$\mathbf{E}_s(\mathbf{R}) = \frac{E_0}{4\pi\epsilon_0 R_0} e^{ik_s R_0} \mathbf{k}_s \times \left[\mathbf{k}_s \times \int d^3 r e^{i\mathbf{q}\cdot\mathbf{r}} \delta\bar{\epsilon}(\mathbf{r})\right] \cdot \hat{n}_0. \tag{1}$$

Here ϵ_0 is the average medium dielectric constant, $\mathbf{k}_s$ is the scattered propagation vector, and $\mathbf{q} = \mathbf{k}_0 - \mathbf{k}_s$ is a measure of the difference between the $\mathbf{k}_0$ and $\mathbf{k}_s$, primarily as a function of the scattered angle.

It is important to note that the overall contribution to the scattered electric field comes about from the integral involving $\mathbf{q}$ in the phase factor $\exp(i\mathbf{q} \cdot \mathbf{r})$. Since $\mathbf{q}$ is only a function of the relative angle between the incident and the scattered field directions in this space, results are general and applicable to any angle of incidence. It is only when these results are transformed to the laboratory fixed system that the change of the direction of $\mathbf{k}_0$ will lead to changes of the scattered or diffracted field. Consequently, we shall discuss the results as much as possible in the $\mathbf{q}$-space or reciprocal space. It should be noted that the integral over all elements of the fiber subject to the phase factor $\exp(i\mathbf{q} \cdot \mathbf{r})$ is analogous to operating in the

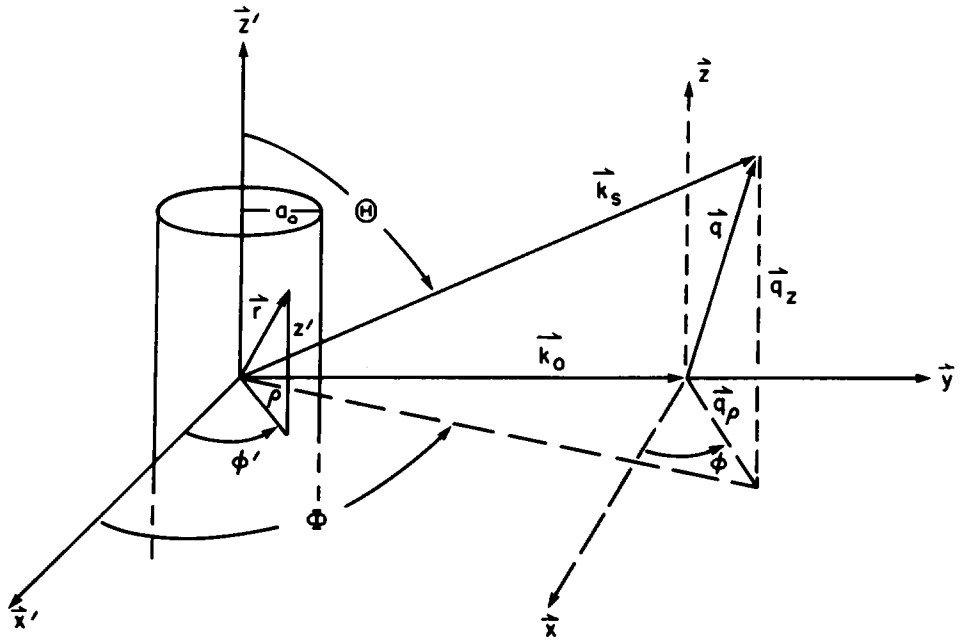

FIGURE 1 Diagram of the uniform cross-section model of a myofibril aligned with axis along the z-direction. Incident wavevector, $\mathbf{k}_0$, is along y-direction, and scattered (diffracted) wave direction, $\mathbf{k}_s$, is at angle (Φ, θ) with respect to the fiber origin. Note $\mathbf{q} = \mathbf{k}_s - \mathbf{k}_0$.

reciprocal Fourier space, the latter leading to the Ewald sphere for satisfying Bragg reflection conditions.

Since it is well known that a purely sinusoidal grating can diffract light only into a single angle via single scattering processes, it is most useful to decompose the striation pattern into all its possible Fourier components. Thus, the dielectric function takes on the general form:

$$\delta\bar{\epsilon}(\mathbf{r}) = Re\left(\sum_{\ell} \delta\bar{\epsilon}_{0_\ell} e^{-i\ell Kz'}\right), \tag{2}$$

where K is the Fourier period of the cylinder lattice, its spacing being given by $\Lambda = 2\pi/K$, and $\delta\bar{\epsilon}_{0_\ell}$ is the dielectric function maximum associated with the ℓ^{th} Fourier component.

In the present case the basic dielectric cylinder is a myofibril of radius a_0. Consider the schematic diagram of Fig. 2 as a small cross-sectional region of the single fiber. This region is composed of many myofibrils whose cross-sectional area, πa_0^2, is assumed to have a constant dielectric value. Since each myofibril spans the entire z-direction where the dielectric constant varies periodically, the full characterization of a point in the system is given by

$$\mathbf{R}_{mu} = \mathbf{R}_0 - (\mathbf{r}_m + \mathbf{r}_{mu}), \tag{3}$$

where $\mathbf{r}_{mu}$ denotes the location within the $\mathbf{m}^{\text{th}}$ myofibril. $\mathbf{r}_m$ denotes the position of the m^{th} myofibril with respect to a reference myofibril of the system, which is at a point $\mathbf{R}_0$ away from the detector. In this representation, the dielectric function for the m^{th} myofibril is given by

$$\delta\bar{\epsilon}_m(r_{mu}) = Re\left[\sum_{\ell} \delta\bar{\epsilon}_{0_\ell} e^{-i(\ell K z_{mu} + \phi_m)}\right], \tag{4}$$

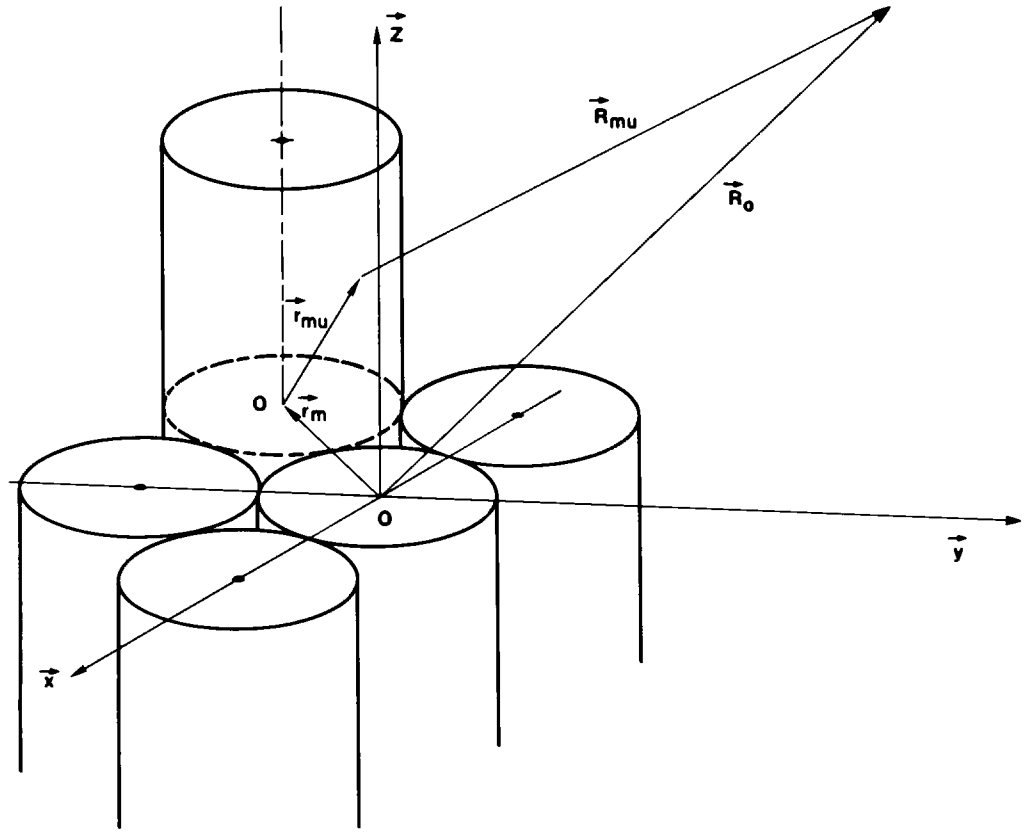

FIGURE 2 Diagram of a small part of cross-sectional view of the fiber which is composed of myofibrils. Each myofibril has radius a_0. The field from the u^{th} elemental region of the m^{th} myofibril is located by $\mathbf{R}_{mu} - \mathbf{R}_0 - (\mathbf{r}_m + \mathbf{r}_{mu})$. Note particularly that $\mathbf{r}_m$ lies only in the cross-sectional plane of the fiber.

where ϕ_m is the phase shift of the m^{th} myofibril relative to an arbitrarily chosen reference myofibril. The scattered field at the detector from all of the myofibrils becomes

$$\mathbf{E}_s(\mathbf{R}) = \frac{E_0}{4\pi\epsilon_0 R_0} e^{ik_s R_0} \mathbf{k}_s \times \left[\mathbf{k}_s \times \sum_m \sum_\ell \int d^3 r_{mu} e^{i\mathbf{q}\cdot(\mathbf{r}_{mu}+\mathbf{r}_m)} \delta\bar{\epsilon}_{0_\ell} e^{-i(\ell K z_{mu}+\phi_m)} \right] \cdot \hat{n}_0. \quad (5)$$

Consider the field resulting from the ℓ^{th} order alone:

$$\mathbf{E}_{s_\ell}(\mathbf{R}) = \frac{E_0}{4\pi\epsilon_0 R_0} e^{ik_s R_0} \mathbf{k}_s \times \left[\mathbf{k}_s \times \sum_m e^{i(\mathbf{q}\cdot\mathbf{r}_m - \phi_m)} \delta\bar{\epsilon}_{0_\ell} \int d^3 r_{mu} e^{i(\mathbf{q}\cdot\mathbf{r}_{mu} - Kz_{mu})} \right] \cdot \hat{n}_0. \quad (6)$$

The integral over the myofibril volume is composed of two parts: the radial contribution of the myofibril and the z-dimension striation, each independent of the particular m^{th} myofibril specification. Upon evaluation (Appendix), we have

$$\int d^3 r_{mu} e^{i(\mathbf{q}\cdot\mathbf{r}_{mu} - Kz_{mu})} = \frac{p \sin (q_z - \ell K)\frac{p}{2}}{(q_z - \ell K)\frac{p}{2}} F(q_\rho a), \tag{7}$$

where

$$F(q_\rho a) \equiv \frac{2\pi a_0}{q_\rho} J_1(q_\rho a_0) \tag{8}$$

is the scattering function in the azimuthal direction and q_z and q_p are as defined according to Fig. 1 and the Appendix. The term of the form $\sin xp/xp$, representing the field pattern due to the z-direction sinusoidal grating, tends toward a Dirac δ-function as the size of the beam, p, tends toward infinity.

$$\lim_{p\to\infty} 2\left[\frac{\sin (q_z - \ell K)\frac{p}{2}}{(q_z - \ell k)}\right]\frac{2\pi}{q_z}\delta\left(1 - \frac{\ell K}{q_z}\right). \tag{9}$$

Substituting the result of Eq. 7 back into Eq. 6, we have

$$\mathbf{E}_{s_t}(\mathbf{R}) = \frac{E_0}{4\pi\epsilon_0 R_0} e^{ik_s R_0}\mathbf{k}_s \times \left[\mathbf{k}_s \times \frac{p \sin (q_z - \ell K)\frac{p}{2}}{(q_z - \ell K)\frac{p}{2}} F(q_\rho a_0)\delta\bar{\epsilon}_{0_t}\sum_m e^{i(\mathbf{q}\cdot\mathbf{r}_m - \phi_m)}\right]\cdot\hat{n}_0. \tag{10}$$

Eq. 10 represents the most general case for the field at the diffraction peak of the ℓ^{th} order. Three cases will be dealt with in the present study: all myofibrils are in phase (case I); myofibrils are systematically skewed in phase (case II); and myofibril phasing is random in a Gaussian approximation (case III).

Case I

If all of the myofibrils were in register, then $\phi_m = 0$

$$\sum_m e^{i\mathbf{q}\cdot\mathbf{r}_m} \to \int_{\text{Fiber}} e^{iq_\rho r}\, dr = F(q_\rho a), \tag{11}$$

where a is the radius of the whole fiber. Substituting Eq. 11 into Eq. 10 and using the approximation (8) that $F(q_\rho r) \sim e^{-q_\rho r}$, we have

$$\mathbf{E}_{s_t}(\mathbf{R}) = \frac{E_0}{4\pi\epsilon_0 R_0} e^{ik_s R_0}\mathbf{k}_s \times \left[\mathbf{k}_s \times \frac{p \sin (q_z - \ell K)\frac{p}{2}}{(q_\rho - \ell K)\frac{p}{2}} F(q_\rho a)\delta\bar{\epsilon}_{0_t}\right]\cdot\hat{n}_0. \tag{12}$$

Here the diffraction field is that arising from the total fiber. For the isotropic contribution, the

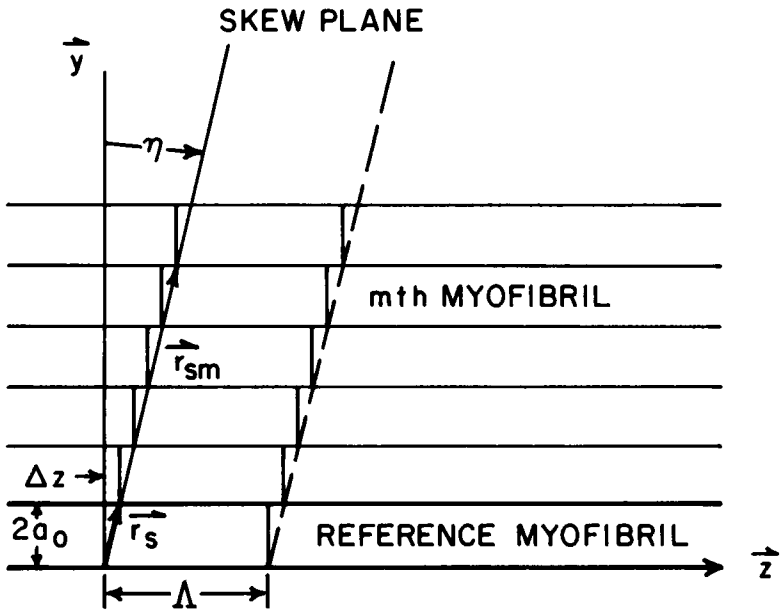

FIGURE 3 Diagram of a skewed arrangement of myofibrils, each of which is composed of sarcomeres of length Λ along the z-axis. The skew plane, as defined by the angle η, satisfies the condition $\tan\eta = \Delta z/2a_o$.

intensity of the ℓ^{th} order becomes

$$I_\ell(\mathbf{R}) = \left(\frac{E_0}{4\pi\epsilon_0 R_0}\right)^2 \left[\frac{p \sin (q_z - \ell K)\frac{p}{2}}{(q_\rho - \ell K)\frac{p}{2}}\right]^2 |F(q_{\rho_t} a)|^2 |\delta\epsilon_{0_t}|^2. \tag{13}$$

This is the case discussed in our previous paper (1).

Case II

If myofibril skewness does exist but there is only one skew plane (Fig. 3), then ϕ_m may be simplified for all myofibrils relative to an arbitrary reference myofibril. From Fig. 3 it is seen that

$$\phi_m = \mathbf{q} \cdot \mathbf{r}_{sm}, \tag{14}$$

where $\mathbf{r}_{sm}$ is the lattice shift of the m^{th} myofibril (Fig. 3). If the reference myofibril has its reference plane located at the point $\mathbf{r}_0$ and the skew plane lies along $\mathbf{r}_s$, then $\mathbf{r}_{sm} = m\mathbf{r}_s$.

The intermyofibril phase becomes $\exp[i\mathbf{q} \cdot (\mathbf{r}_0 - m\mathbf{r}_s)]$, and the summation of these phase factors gives rise to

$$\sum_m e^{i\mathbf{q}\cdot(\mathbf{r}_0 - m\mathbf{r}_s)} = e^{i\mathbf{q}\cdot\mathbf{r}_0} \sum_{m=1}^{N} e^{-i(\mathbf{q}\cdot\mathbf{r}_s)m}. \tag{15}$$

This sum over N myofibrils can be calculated, and it leads to

$$\sum_{m=1}^{N} e^{-imA} = \frac{\sin \frac{NA}{2}}{\sin \frac{A}{2}}, \tag{16}$$

where

$$A \equiv \mathbf{q} \cdot \mathbf{r}_s. \tag{17}$$

The scattered field now contains a new interference term (Eq. 11), and we have

$$\mathbf{E}_{s_q}(\mathbf{R}) = \frac{E_0}{4\pi\epsilon_0 R_0} e^{ik_s R_0} \mathbf{k}_s \times \left[\mathbf{k}_s \times \frac{p \sin (q_z - \ell K) \frac{p}{2}}{(q_z - \ell K) \frac{p}{2}} F(q_\rho a_0) \delta \bar{\epsilon}_{0_q} e^{i(\mathbf{q}_s \cdot \mathbf{r}_i - \ell K_s)} \frac{\sin \frac{NA}{2}}{\sin \frac{A}{2}} \right] \cdot \hat{n}_0 \tag{18}$$

Again, if we consider only linear incident polarization and the isotropic component of the dielectric function, we obtain for the intensity of the ℓ^{th} order diffraction pattern:

$$I_\ell(\mathbf{R}) = \frac{|E_0|^2 |\delta\epsilon_{0_q}|^2}{(4\pi\epsilon_0 R_0)^2} \left[\frac{p \sin (q_z - \ell K) \frac{p}{2}}{(q_z - \ell K) \frac{p}{2}} \right]^2 |F(q_\rho a_0)|^2 \left[\frac{\sin^2 \left(\frac{NA}{2} \right)}{\sin^2 \left(\frac{A}{2} \right)} \right]. \tag{19}$$

Eq. 19 describes the normal incidence diffraction from a single fiber which exhibits a skew plane along $\mathbf{r}_s$, uniformly across the entire region of illumination, p.

Case III

Instead of systematic skewing of the myofibrils as discussed in Case II, we consider the situation where the myofibrils are randomly out of register with respect to adjacent myofibrils. Here, the ordered phase shifts, $\mathbf{q} \cdot m\mathbf{r}_s$, goes over to a random phase shift, ϕ_m, where m, as before, indicates the m^{th} myofibril. If ϕ_m were a Gaussian random variable, we can assume that the phasing between neighboring myofibrils is represented by the probability function

$$P(\phi) = \frac{1}{\sqrt{2\pi\sigma_\phi^2}} \exp \left[-\frac{\phi^2}{2\sigma_\phi} \right], \tag{20}$$

where σ_ϕ is the standard deviation for random phasing, and if σ_ϕ is large compared with the $\Delta z / 2a_0$, we can then ignore the skew planes and treat the random phase problem by letting

$$\sum_m e^{i\phi_m} \rightarrow \int_{-\infty}^{\infty} P(\phi) e^{i\phi} \, d\phi. \tag{21}$$

Evaluation of this integral leads to

$$\sum_m e^{i\phi_m} \sim e^{-\sigma_\phi^2/2}.$$

The ℓ^{th} diffraction intensity can now be given by

$$I_\ell(\mathbf{R}) = \frac{|E_0|^2 |\delta\epsilon_{0_\ell}|^2}{(4\pi\epsilon_0 R_0)^2} \left| \frac{p \sin (q_z - \ell K) \frac{p}{2}}{(q_z - \ell K) \frac{p}{2}} \right|^2 |F(q_\rho a_0)|^2 e^{-\sigma_\phi^2}. \quad (22)$$

It is of interest to note that the Bragg condition of Eq. 19 is now replaced by a damping term, $e^{-\sigma_\phi^2}$, depending on the breadth of the spread of myofibril phasing. The signals become more symmetrical with respect to left and right peaks of the same diffraction order but do not spread in their meridional plane. Under this type of myofibril randomization, the specific sarcomere A-I band relationship has not been destroyed. The decrease in intensity as a result of the dephasing factor, exp $[\sigma_\phi^2]$, applies uniformly throughout all orders of the diffraction pattern. Furthermore, the basic azimuthal pattern is reflective of the myofibril diameter, not the whole fiber.

It should be noted that the case treated here (III) is not similar to the randomization discussed by Fujime (6). In that situation only A-band randomization of each sarcomere is considered. As a result, the relative A-I band positions are randomized. Consequently, Fujime predicts differences in the intensity decrease as a function of diffraction order.

DISCUSSION

The present theory leads to several interesting conclusions. One principal result is that since a single fiber is of dimensions ~100 μm across its diameter, the three-dimensional nature of this grating must be fully considered. Eq. 13 shows that the observed intensity at any particular diffraction order of the grating, given by $q_z = \ell K$, is modulated by the factor $F(q_{\rho_\ell} a)$, describing the transmission of light through the thickness of the fiber at any particular diffraction angle. As a consequence, electric field interference at a point of detection comes from not only the individual myofibril grating, but also from the bundle of myofibril, each at its specific location. Such compound interference and diffraction were examined for two different myofibril dielectric function representations by Baskin et al. (1), and their results for the passively stretched fiber exhibit the sensitivity of the diffraction pattern to different myofibrils' model representations. In particular, second order diffraction peak intensity is very sensitive to the presence of H-band or Z-membrane. This result is related to the fact that both the H-band and the Z-membrane together reinforce the second harmonic contribution of the grating. Su and Gaylord (9) in their recent study of diffraction efficiencies of thick grating arrived at the same conclusion, even though their treatment was not limited to single scattering process.

A second contribution to higher order diffraction intensities comes from multiple scattering processes. For a thick grating where the probability of secondary scattering is high, the diffracted light via single scattering process can be scattered again before leaving the fiber.

Because the fiber retains the basic periodicity structure, the location of secondary scattered light intensity peaks is nearly identical to the position of intensity maxima from primary scattering. However, this type of mode-coupling (10) essentially feeds higher order intensity lobes at the expense of the first order. Theoretical studies of this type data back to Raman and Nath (11, 12). Considering only normal incidence situation and a nonskewed, simple harmonic grating structure, the theory of Raman and Nath predicts $(I_2/I_1) \simeq 0.02$ when the muscle parameters are used (1). Both Eq. 13 and the Raman-Nath result are based on the idea of a transmission grating. Neither theory seems to be able to predict the much larger (~10%) second order diffraction intensity observed in our earlier publication (1). We next turn to reflection gratings.

Bragg reflection, as shown in the previous section, provides a further source of signal enhancement and intensity asymmetry. Each of these two aspects deserves some attention.

The result of the present theory in Case II is given by Eq. 19. Since the term $[\sin(NA/2)/\sin(A/2)]^2$ has an absolute maximum of N^2 at the Bragg condition ($A = 0$), the intensity, I_ℓ, only attains its theoretical maximum when this condition is satisfied. Whenever $A \neq 0$, this modulation function on the diffraction is very much less than the $A = 0$ value; correspondingly, the intensity decreases. For the normal incidence situation, and if we further consider that the skew plane lies in the plane of $\Phi = \pi/2$, then the Bragg condition, $A = 0$, and the sarcomere diffraction condition will be simultaneously satisfied at the ℓ^{th} order only when

$$q_{z_\ell} = \ell K, \tag{23}$$

and

$$q_{\rho_\ell} = \frac{(\ell K)^2}{2k_0}. \tag{24}$$

Fig. 4 provides a detailed intensity representation for the situation considered. The phase factor A is plotted against the skewness Δz for families of diffraction patterns at the various representative orders (ℓ) and differing sarcomere lengths (Λ). The intersection of these lines at the $A = 0$ is the Bragg condition for those particular orders. One notices that when, for example, $\ell = 1$, $\Lambda = 2.0$ μm satisfies $A = 0$, $\Delta z = -0.12$ μm. The corresponding A value for the negative order ($\ell = -1$, $\Lambda = 2.0$ μm) is ~0.75. For $N = 100$ and $A = 0.75$ $[\sin(NA/2)/\sin(A/2)]^2$ is $\sim 10^{-3}$ down from the peak value of N^2. Consequently, this theory predicts intensity asymmetry when the Bragg condition is fulfilled for a given order of diffraction.

Several other features are also important to recognize. If the Bragg reflection condition is not completely satisfied, such as the case when $\Delta z = -0.5$ μm, one has a rather different set of intensity ratios. For $\Lambda = 3.0$ μm, the intensity peaks of the first order right ($+1$) to the first order left (-1) to the second order right ($+2$) is given by $1:-1:2 = 573:10.5:14.5$. This result suggests that as soon as the Bragg condition is not fully met, the degree of intensity asymmetry between left and right decreases dramatically. Furthermore, the second order peak ($+2$) constitutes ~3% of the intensity of the first order peak ($+1$). A comparison of the present theory with the coupled-mode theory by Magnusson and Gaylord (10) shows that a 3% ratio between second order and first order is again fairly consistent given the simply harmonic grating adjusted to the parameters of the muscle sarcomere. Even when a "square

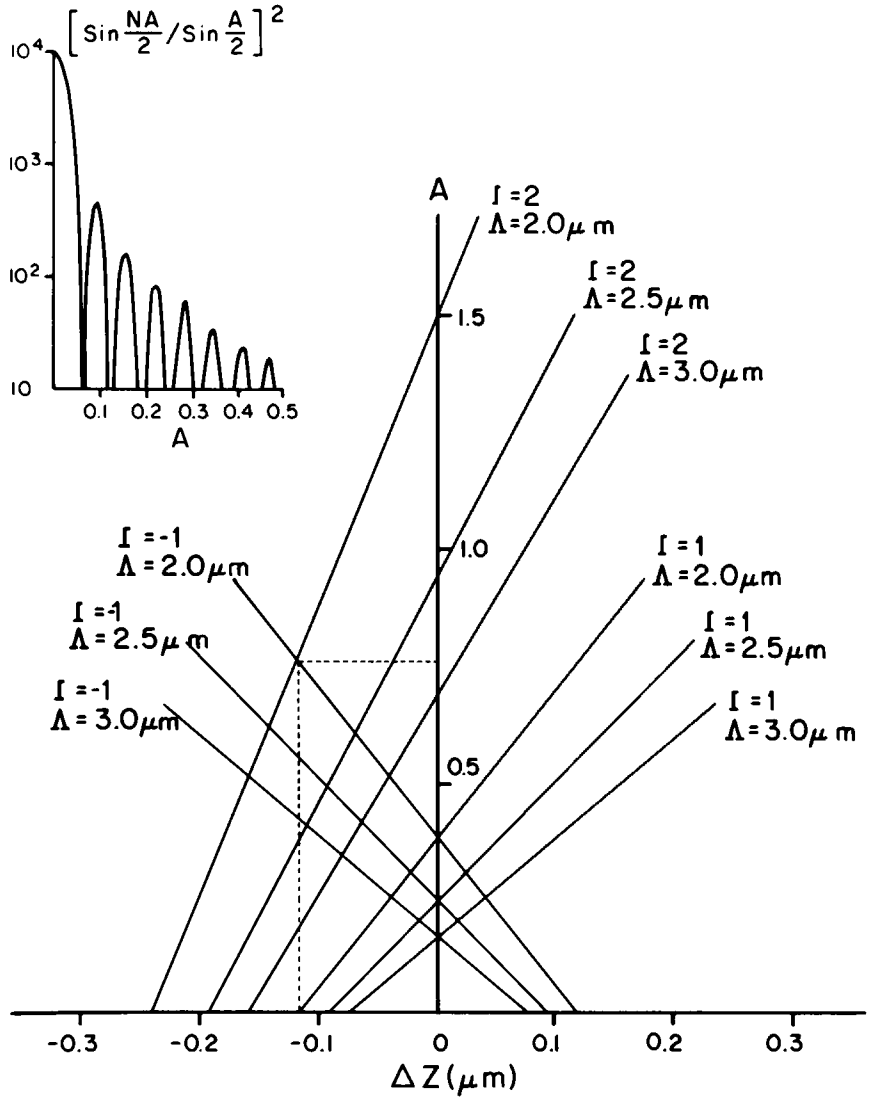

FIGURE 4 Plot of $A = \mathbf{q} \cdot \mathbf{r}_s = \ell K[\Delta z + zKa_0/\ell k_0]$ vs. Δz as a function of ℓ and $\Lambda = 2\pi/K$. $a_0 = 0.5$ μm is used. $k_0 = 2\pi n_0/\lambda_0$ where $\lambda_0 = 0.633$, $n_0 = 1.334$. Bragg condition is indicated at $A = 0$ for the various orders. In the insert, $[\sin(NA/2)/\sin(A/2)]^2$ is plotted vs. A for $N = 100$.

wave type" grating is considered, Magnusson and Gaylord's results show that the ratio does not alter appreciably at these $\delta\epsilon_0$ differences. Thus, the mode-coupling theory does not seem to predict very much excessive dumping of intensities from one order to the next when $\delta\epsilon_0$ is taken to be that of the muscle A-I band differential.

A further point to be noted from Fig. 4 is that there may be large skewness parameters such that the first order Bragg condition can no longer be satisfied for a given order. Under those conditions higher order Bragg conditions might be considered. We shall not go into these large angle diffraction problems here.

When a qualitative comparison of the present result based on Eq. 19 is made with the experimental observations of Rudel and Zite-Ferency (3) for their case of normal laser incidence ($\omega = 0$), we find that the experimental results exhibit a smaller ratio of the intensity asymmetry than the pure Bragg reflection result of the present theory. On the other hand, it is not possible to say definitively what the origin of this smaller asymmetry ratio is. Either the non-Bragg conditions which we have just described, or the fact that the real system contains smaller domains of fewer Bragg planes would tend to reduce the asymmetry ratio.

The $A = 0$ condition for any order leads to

$$\ell K = 2k_0 \tan \eta, \tag{25}$$

where η is the angle of the skew plane, defined by

$$\tan \eta = \frac{\Delta z}{2a_0}. \tag{26}$$

Eq. 25 clearly shows that the $+\ell$ and $-\ell$ order diffraction patterns satisfy the Bragg condition at different values of skewness; consequently, there is, distinctively, intensity asymmetry. Eq. 25 may further be written as

$$2\Lambda \tan \eta = \frac{\ell \lambda_0}{n_0} \tag{27}$$

for comparison with the theory of Rudel and Zite-Ferency (2). In their case, a continuum of grating points is assumed to exist on the Bragg planes; present work assumes that skewing takes place only between myofibrils, while the individual sarcomere period planes are still perpendicular to the myofibril axis. The two results agree in the limit of small angle η. For small η, $\tan\eta \approx \eta$. Therefore, $2\tan\eta \approx \sin 2\eta$; thus, Eq. 27 becomes the Rudel and Zite-Ferency result. Such an agreement exists because under the small η condition, the distinction of the sarcomere arrangement within the myofibril tends toward the continuum of grating points.

Present theory also shows that when $\Delta z = 0$, the left and right orders are identical in intensity, and one recovers the results of Eq. 13. In addition, this theory contains the complete description of the diffraction pattern in the azimuthal plane. Specifically, the theory suggests that the cross-section of the myofibril, not the whole single fiber, will be the major contributor to the azimuthal pattern in the presence of myofibril skewness.

The discussion for normal incidence, k_0, can easily be generalized to arbitrary incident angle with respect to the fiber. An in-depth study of single fiber diffraction under these conditions, both theoretically and experimentally, is under way and will be reported separately.

Randomization of myofibril phases is another observation of considerable interest. Bonner and Carlson (13) showed that many elements with diameters of the myofibril seem to undergo independent random changes in their axial positions during the plateau of an isometric tetanus. Paolini et al. (14) had further shown that when the muscle is subjected to an isometric twitch stimulation, whereas neither the diffraction position nor the line shape changes noticeably, the diffraction intensity does decrease appreciably. The present theory provides a qualitative description of these experimental observations. If within the laser illumination region the lengths of the sarcomeres do not vary in length, then Eq. 22 provides a

description of how the intensity decreases due strictly to myofibril phase randomization. In Fujime and Yoshino's most recent work (5), the random variation of sarcomere length within a given myofibril was treated as a Debye-Waller factor. These authors, however, did not discuss whether or not the intensity decrease in their case is accompanied by a change in the line shape. It had previously been shown by Morgan (15) that should there be two distinctively different populations of sarcomeres sampled by the laser beam, there indeed will be a complex meridional diffraction pattern at any order. Since the results of Paolini et al. (14) do not suggest such additional structure during contraction, it seems that myofibril phase randomization is a more plausible explanation for diffraction intensity changes in these observations.

LIST OF SYMBOLS

a Radius of single fiber.
a_0 Radius of myofibril.
E_0 Magnitude of incident electric field.
$\mathbf{E}_s$ Scattered electric field at the field point.
ϵ_0 Average medium dielectric constant.
$\delta\tilde{\epsilon}_{0_\ell}$ Magnitude of ℓ^{th} Fourier component of dielectric fluctuation.
η Angle of the skew plane.
I_s Scattered intensity.
K Fourier period of cylinder along z-axis.
$\mathbf{k}_0$ Incident light wavevector.
$\mathbf{k}_s$ Scattered light wavevector.
ℓ Index of the Fourier spectrum order. Also, order of diffraction.
Λ Length of sarcomere.
λ_0 Incident light wavelength in vacuum.
n_0 Average material index of refraction.
$\hat{n}_0$ Incident light polarization direction.
N Number of myofibrils.
p Spatial extent radius of the incident beam.
$\mathbf{q}$ Difference between incident and scattered wavevectors.
$\mathbf{q}_\rho$ Radial component of $\mathbf{q}$.
$\mathbf{q}_z$ Z-component of $\mathbf{q}$.
$\mathbf{R}$ Field point from a particular element of scatterer.
$\mathbf{R}_{mu}$ Field point from u^{th} element of the m^{th} myofibril.
$\mathbf{R}_0$ Field point for observation from center of scatterer.
$\mathbf{r}$ Location of a point within material (fiber or myofibril).
$\mathbf{r}_m$ Location of center of m^{th} myofibril.
$\mathbf{r}_{mu}$ Location of u^{th} element of scatterer of the m^{th} myofibril.
$\mathbf{r}_0$ Location of reference myofibril.
$\mathbf{r}_s$ Basis vector for the skew plane.
σ_ϕ Variance of phase ϕ.
Φ Angle of diffraction in the horizontal plane.
ϕ_m Phase of m^{th} myofibril with respect of $z = 0$ plane.
Δz Z-component of the myofibril skewness.

APPENDIX

Evaluation of the Diffraction Integral of a Striated Cylinder

To carry out the integral evaluation of Eq. 6, it is necessary to decompose the $\mathbf{q}$ and $\mathbf{r}$ vectors in terms of coordinates convenient for the cylindrical geometry. Following the notations of Fig. 1,

$$\mathbf{q} = q_\rho \cos\phi\hat{x} + q_\rho \sin\phi\hat{y} + q_z\hat{z}, \tag{A1}$$

$$\mathbf{r} = \rho \cos\phi'\hat{x} + \rho \sin\phi'\hat{y} + z'\hat{z}, \tag{A2}$$

Consequently,

$$\mathbf{q} \cdot \mathbf{r} = q_\rho\rho \cos(\phi' - \phi) + q_z z'. \tag{A2}$$

Substituting Eq. A2 into the integrand of Eq. 6, one obtains, for the radial part of the integral, $\int_0^{a_0} \rho d\rho \int_0^{2\pi} e^{iq_\rho\rho\cos(\phi'-\phi)}d\phi'$, where a_0 is the radius of the myofibril. The (ϕ', ρ) integrations lead to the well-known expression for scattering by a homogeneous cylinder (16):

$$\int_0^{a_0} \rho d\rho \int_0^{2\pi} e^{iq_\rho\rho\cos(\phi'-\phi)}d\phi' = \frac{2\pi a_0^2}{q_\rho a_0} J_1(q_\rho a_0) \equiv F(q_\rho a_0) \tag{A3}$$

$J_1(x)$ being the Bessel function of first order. The z' integration over the dimensions of the incident beams, $\pm p/2$, is also well known,

$$\int_{-p/2}^{p/2} dz' e^{i(q_z - \ell K)z'} = \frac{p \sin(q_z - \ell K)\frac{p}{2}}{(q_z - \ell K)\frac{p}{2}}. \tag{A4}$$

Combining the results of Eqs. A3 and A4, Eq. 7 of the text is arrived at.

To further specify q_ρ and q_z, the scattered wavevectors along the ρ and $\mathbf{z}$ directions must be related to laboratory oriented coordinates. For the normal incidence case,

$$|q_\rho| = [(k_s \sin\Theta\cos\Phi)^2 + (k_s \sin\Theta \sin\Phi - k_0)^2]^{1/2} \tag{A5}$$

and at the peak of the ℓ^{th} diffraction pattern, $q_z = \ell K$. Since $|k_s| \sim |k_0|$, we have

$$q_{z_\ell} = \ell K = k_0 \cos\Theta_\ell \tag{A6}$$

and

$$q_{\rho_\ell} = k_0\left[(1 - \sin\Phi)\left(2 - \left(\frac{\ell K}{k_0}\right)^2\right) + \frac{\sin\Phi}{4}\left(\frac{\ell K}{k_0}\right)^4\right]^{1/2}. \tag{A7}$$

These results are used in Eq. 10.

The authors would like to express their appreciation to the National Science Foundation (grant PCM-77-08371 to Y. Yeh and PCM-79-03256 to R. J. Baskin) for their financial support.

Received for publication 30 November 1978 and in revised form 25 November 1979.

REFERENCES

1. BASKIN, R. J., K. P. ROOS, and Y. YEH. 1979. Light diffraction study of single skeletal muscle fibers. *Biophys. J.*, **28**:45–64.
2. RÜDEL, R., and F. ZITE-FERENCY. 1979. Interpretation of light diffraction by cross-striated muscle and Bragg reflection of light by the lattice of contractile proteins. *J. Physiol.* **290**:317–330.
3. RÜDEL, R., and F. ZITE-FERENCY. 1979. Do laser diffraction studies on striated muscle indicate stepwise sarcomere shortening? *Nature (Lond.)*. **278**:573–575.
4. POLLACK, G. H., T. IWAZAMI, H. E. D. T. TER KERUS, and E. F. SHIBATA. 1977. Sarcomere shortening in striated muscle occurs in stepwise fashion. *Nature (Lond.)*. **268**:757–759.

5. FUJIME, S., and S. YOSHINO. 1978. Optical diffraction study of muscle fibers I.A. theoretical basis. *Biophys. Chem.* **8**:305–315.
6. FUJIME, S. 1975. Optical diffraction study of muscle fibers. *Biochim. Biophys. Acta.* **379**:227–238.
7. BERNE, B. J., and R. PECORA. 1976. Dynamic Light Scattering. John Wiley & Sons, Inc., New York. 33–36.
8. BEAR, R. S., and O. E. A. BOLDUAN. 1950. Diffraction by cylindrical bodies with periodic axial structure. *Acta Cryst.* **3**:236–241.
9. SU, S. F., and T. K. GAYLORD. 1975. Calculation of arbitrary-order diffraction efficiencies of thick gratings with arbitrary grating shape. *J. Opt. Soc. Am.* **65**:59–64.
10. MAGNUSSON, R., and T. K. GAYLORD. 1977. Analysis of multiwave diffraction of thick gratings. *J. Opt. Soc. Am.* **67**:1165–1170.
11. RAMAN, C. V., and N. S. N. NATH. 1935. The diffraction of light by high frequency sound waves. I. *Proc. Ind. Acad. Sci.* (A), 406–412.
12. RAMAN, C. V., and N. S. N. NATH. 1936. The diffraction of light by high frequency sound waves. IV. *Proc. Ind. Acad. Sci.* (A), 119–125.
13. BONNER, R. F., and F. D. CARLSON. 1975. Structural dynamics of frog muscle during isometric contraction. *J. Gen. Physiol.* **65**:555–581.
14. PAOLINI, P. J., K. P. ROOS, and R. J. BASKIN. 1977. Light diffraction studies of sarcomere dynamics in single skeletal muscle fibers. *Biophys. J.* **20**:221–232.
15. MORGAN, D. L. 1978. A prediction of some effects on light diffraction patterns of muscles produced by areas with different sarcomere lengths. *Biophys. J.* **24**:88 *a*. (Abstr.).
16. WATSON, G. N. 1952. A Treatise on the Theory of Bessel Functions. Cambridge University Press, Cambridge. 18, 25, 393.